

# What is the price of abandoning dark matter?

## Cosmological constraints on alternative gravity theories

Kris Pardo<sup>1,2,\*</sup> and David N. Spergel<sup>2,3</sup>

<sup>1</sup>*Jet Propulsion Laboratory, California Institute of Technology, Pasadena, CA 91101, USA*

<sup>2</sup>*Department of Astrophysical Sciences, Princeton University, Princeton NJ 08544, USA*

<sup>3</sup>*Center for Computational Astrophysics, Flatiron Institute, NY NY 10010, USA*

(Dated: July 2, 2020)

Any successful alternative gravity theory that obviates the need for dark matter must fit our cosmological observations. Measurements of microwave background polarization trace the large-scale baryon velocity field at recombination and show very strong,  $O(1)$ , baryon acoustic oscillations. Measurements of the large-scale structure of galaxies at low redshift show much weaker features in the spectrum. If the alternative gravity theory's dynamical equations for the growth rate of structure are linear, then the density field growth can be described by a Green's function:  $\delta(\vec{x}, t) = \delta(\vec{x}, t')G(x, t, t')$ . We show that the Green function,  $G(x, t, t')$ , must have dramatic features that erase the initial baryon oscillations. This implies an acceleration law that changes sign on the  $\sim 150$  Mpc scale. On the other hand, if the alternative gravity theory has a large nonlinear term that couples modes on different scales, then the theory would predict large-scale non-Gaussian features in large-scale structure. These are not seen in the distribution of galaxies nor in the distribution of quasars. No proposed alternative gravity theory for dark matter seems to satisfy these constraints.

### INTRODUCTION

The astronomical evidence for dark matter continues to grow: the velocities of galaxies imply the existence of dark matter in clusters [1, 2]; measurements of rotation curves reveal its presence in galaxies like our own [3–5]; dynamical arguments demonstrate its ubiquity [6]; and gravitational lensing measurements confirm its presence in clusters and galaxies [7, 8]. Cosmological observations provide another line of evidence for the existence of dark matter: the popular  $\Lambda$  Cold Dark Matter ( $\Lambda$ CDM) model is remarkably successful in simultaneously fitting cosmic microwave background (CMB) observations and the large-scale distribution of structure [e.g., 9, 10]. This concordance requires that the dominant form of matter is not baryons but cold, weakly-interacting (or non-interacting) dark matter.

While dark matter and dark energy have become part of the standard paradigm, we have yet to detect dark matter nor do we have a deep physical understanding of the tiny cosmological constant value. With ever improving dark matter experiments ruling out much of the parameter space associated with the “WIMP” miracle [11, 12], there has been renewed interest in alternative gravity theories that obviate the need for dark matter, dark energy, or perhaps even both.

While Occam's razor would prefer a baryons-only universe, it has proven very challenging to develop a satisfactory alternative to General Relativity (GR). Any successful modified gravity theory will need to reproduce the successes of  $\Lambda$ CDM and GR:

1. Provide an explanation for the flatness of galaxy rotation curves at large radii, the distribution of hot gas in elliptical galaxies and clusters of galaxies, and match the gravitational lensing shear mea-

surements;

2. Satisfy the classical tests of GR, including the precession of the perihelion of Mercury and other solar system tests, the Shapiro time delay, and the timing of binary millisecond pulsars [13].
3. Provide a consistent fit to LIGO's gravitational wave signals. These measurements provide strong constraints on the tensor content of any gravitational wave theory [14–17].
4. Predict an expanding universe and provide an acceptable fit to measurements of the distance-redshift relationship. This constrains the homogeneous cosmological solution of the alternative theory [c.f., 18].
5. Provide a satisfactory fit to measurements of both the CMB fluctuations and the large-scale structure.

This Letter quantifies the final constraint on this list: any alternative gravity theory that obviates the need for dark matter needs to provide an explanation for the growth and evolution of structure.

The  $\Lambda$ CDM model accurately explains how structure forms from initial density perturbations and how these perturbations are imprinted in the cosmic microwave background [19–23]. The initial fluctuations are adiabatic: overdense regions have an excess of baryons, dark matter, and photons. In the early universe, the fluctuations in the tightly-coupled baryon-photon fluid oscillate like sound waves. On the other hand, the dark matter is cold and its fluctuations evolve only through gravity. After recombination, baryons decouple from the photons and then fall into the growing dark matter potential wells. This dark matter driven gravitational fluctuation growth

erases most of the signature of the sound waves. Thus, the  $\Lambda$ CDM model can explain why the acoustic oscillations in the cosmic microwave background temperature and polarization fluctuations have  $O(1)$  amplitude and the oscillations in the distribution of galaxies are subtle with amplitude of  $O((\Omega_b/\Omega_m)^2) \sim 0.04$ . *Any alternative gravity theory will have to provide an alternative explanation for this suppression of the acoustic fluctuations, one of the distinctive effects of dark matter.*

In this Letter, we outline how to determine the required infrared (IR) behavior of any dark matter theory based on linking the baryon density field at recombination ( $z \sim 1100$ ) to the baryon power spectrum at low redshift ( $z \sim 0$ ). Any successful theory for dark matter, whether it invokes particles or alternative theories of gravity, must properly explain how the baryon density field at  $z \sim 1100$  evolves into the one at  $z \sim 0$ . These density fields are typically probed indirectly through fitting the CMB power spectra and the matter power spectrum in tandem [e.g., 9, 10]. This necessarily assumes  $\Lambda$ CDM (or some simple extension), as well as GR. The test we propose here does not invoke GR nor a specific cosmology. Instead it relies solely on small-scale physics – Thomson scattering and the Newtonian continuity equation. Note that while similar tests have been proposed before [24, 25], they have not been explicitly formulated nor calculated for general modified gravity theories.

The polarization of the CMB on small scales is exclusively due to Thomson scattering, which itself only relies on the velocities of the electrons. Because protons and electrons are tightly coupled via Coulomb scattering at early times, we can assume that the velocities of the electrons exactly equals that of the protons. The CMB polarization spectrum then directly measures the velocity of the baryons at  $z \sim 1100$ . The Newtonian continuity equation, which is valid at small scales, relates the velocities of the baryons to their density field. Thus, the CMB polarization spectrum is a direct measurement of the baryon velocity field at  $z \sim 1100$ . At  $z \sim 0$ , the galaxy-galaxy correlation function traces the baryon density field at large scales. With these two direct measures of the baryon density field, we can then define the form a linear alternate theory of dark matter must take in the IR. We combine observations of the CMB and the galaxy power spectrum at low-redshift to determine the required Green’s function of structure formation between these redshifts for alternate theories. This Green’s function has a distinctive form as it must suppress the baryon acoustic oscillations by nearly an order of magnitude, as well as greatly increase power on small scales.

Below we describe the theoretical framework for determining the IR behavior of modified gravity theories for dark matter. We first outline the general idea behind our method, which will depend on the baryon power spectrum at both  $z \sim 0$  and  $z \sim 1100$ . We then describe how we calculate each of these power spectra. Finally,

we give the resulting necessary form for an alternative dark matter theory and conclude.

## INFRARED BEHAVIOR OF MODIFIED GRAVITY

We assume that the modified gravity theory predicts our universe is expanding with a scale factor,  $R(t)$ , determined by its dynamical equations and that the form of  $R(t)$  fits the current measurements of the distance-redshift relation. This assumption already places a very profound constraint on any alternative to GR. Here we focus on the evolution of fluctuations on large-scales and in the linear regime.

As is usual in cosmology, we represent the density field as the sum of a mean density field,  $\rho(t)$ , and spatial fluctuation:

$$\rho(\vec{x}, t) = \rho(t) [1 + \delta(\vec{x}, t)] , \quad (1)$$

and expand the density field in Fourier modes:  $\delta(\vec{k}, t)$ , where  $\vec{k}$  is an angular wavevector.

In alternative gravity theories, the acceleration encodes the deviation from GR – these theories generally assume matter and momentum conservation. Thus, we will also assume these conservation laws hold. In agreement with the cosmological principle and observations of large scale structure, we will also assume that any modifications to GR must be isotropic.

We assume that the acceleration in the modified gravity theory only depends on the amplitude of the baryon density fluctuations:  $\vec{a}(\delta_b)$ . We then expand the function as a series of sums of Fourier modes:

$$a(k, t) = \hat{F}_1(k) \delta_b(k, t) + \sum_{k'} \hat{F}_2(k, k') \delta_b(k, t) \delta_b(k', t) + \dots \quad (2)$$

where  $k \equiv \|\vec{k}\|$ ,  $\hat{F}_1(k)$  is the linear response to the density fluctuation (including both GR and modified terms), and  $\hat{F}_2$  encodes the second order correction.

Since the density field is small, the linear term should dominate the gravitational acceleration in most modified gravity theories. Thus, we focus on linear modifications to GR in this paper. Note that this linear term acts like a transfer function – it has no explicit time dependence and is simply multiplied with a given density configuration in  $k$ -space to give the resulting acceleration force.

If the modified gravity theory has strong nonlinear terms, then the theory will produce significant mode-mode couplings that would be apparent in the large-scale structure. The theory could evade the current strong constraints from Planck on non-Gaussianity [26] if the theory is linear at early times. However, if the theory is nonlinear enough at late times to erase the baryon acoustic oscillations, then these same nonlinearities would induce

large non-Gaussian features in the large-scale distribution of structure. These are not seen in the large-scale distribution of structure [27] and they will be further constrained by upcoming missions, such as SphereX<sup>1</sup> [28]. Thus, it is unlikely that a strongly nonlinear theory could produce the correct evolution for the baryons and evade low-redshift non-Gaussianity constraints. Detailed calculations showing this point are left to future work.

## LINEAR MODIFICATION TO GENERAL RELATIVITY

In this section, we constrain the properties of a linear modification to GR. We show that the combination of CMB polarization measurements and large-scale structure determine the form of the transfer function for the growth of baryon fluctuations. This then determines the form of the acceleration equation in any linear modified gravity theory for dark matter.

In  $\Lambda$ CDM after recombination, baryons fall into the dark matter potentials. This imprints the large-scale distribution of the dark matter on the baryons. Thus, the transfer function of CDM, along with the initial spectrum of fluctuations, is all that is needed to accurately describe the matter power spectrum. The baryon power spectrum follows directly by using the CDM potential created by the evolution of these perturbations. However, if we no longer have CDM in our model, the baryon transfer function itself must encode all of this information. *In modified gravity theories of dark matter, the baryon transfer function must account for all of the changes in the baryon perturbations from early to late times.*

The matter power spectrum depends on the transfer function as:  $P(k) \propto P_\phi(k)T^2(k)$ , where  $P_\phi$  is the primordial spectrum of perturbations. In analogy to this, we can define the transfer function:

$$\hat{T}_b^2(k) = \frac{P_{bb}(k, z \sim 0)}{P_{bb}(k, z = 1100)}. \quad (3)$$

$\hat{T}_b^2(k)$  describes how the baryon perturbations evolve from  $z = 1100$  to  $z \sim 0$ . We use the hat here indicate the different normalization from the typical transfer function used in cosmology.

Any theory for dark matter must adequately explain both the shape and normalization of  $\hat{T}_b^2(k)$ . Our transfer function can be exactly represented with measurable data and does not rely on any assumptions about underlying theories, outside of the small-scale physics described below. It is also possible to find the theoretical solutions for any dark matter or modified gravity theories. In this paper, we will focus solely on the shape of  $\hat{T}_b^2(k)$  – a more

precise analysis is required to use the normalization as well.

As a way of building intuition, we will also consider the Fourier pair of the transfer function – the Green’s function:

$$\hat{G}_b(r) = G_0 \int dk \frac{k^2}{2\pi^2} \hat{T}_b(k) j_0(kr), \quad (4)$$

where  $j_0(x)$  is a Spherical Bessel function of the first kind and  $G_0$  is a normalization term that we arbitrarily set such that  $\hat{G}(r = r_{\min}) = 1$ . Here  $r_{\min}$  is the minimum physical radius resolvable from the data. This functions shows, in real space, the inherent acceleration response of the modified gravity.

## The Baryon Power Spectrum at $z \sim 0$

The baryons at low redshift and large scales ( $\gtrsim 10$  Mpc) are well-traced by galaxies. Thus, we can take the 3D power spectrum of galaxies as the baryon power spectrum. This is given by:

$$P_{bb}(k, z \sim 0) = b_{bg}^2 P_{gg}(k, z \sim 0), \quad (5)$$

where  $b_{bg}$  is the bias of baryons relative to galaxies and  $P_{gg}$  is the 3D galaxy-galaxy power spectrum.

In reality, the galaxies are a biased tracer of the baryons. Most of the baryonic mass in the universe is in gas [29]. However, we expect that for  $k < 0.1 \text{ Mpc}^{-1}$  the bias,  $b_{bg}$ , approaches some constant value. This is seen in numerical simulations [e.g., 30] and violating this would require moving baryons large distances. Thus, the galaxy-galaxy power spectrum should be a good measure of the shape of the baryonic power spectrum at these large scales.

We use the data from Ref. [31] for the galaxy-galaxy power spectrum at low- $z$ . Ref. [31] measures the BAO signal from galaxies from  $z = 0.2 - 0.75$  using the Sloan Digital Sky Survey-III [SDSS-III; 32] Baryon Oscillation Spectroscopic Survey (BOSS) DR12 data set [33, 34]. As part of this measurement, they also calculate the 3D galaxy-galaxy power spectrum in 3 different redshift bins. We use the lowest redshift bin,  $z = 0.2 - 0.5$ , which has an effective redshift of  $z = 0.38$ . This is measured from  $k = 0.016 - 0.15 \text{ h Mpc}^{-1}$ . We use their fiducial value of  $h = 0.676$  to transform to physical units.

## The Baryon Power Spectrum at $z \sim 1100$

The polarization of the CMB can be related to the velocity of the baryons as [36]:

$$\Delta_p(\hat{n}, \vec{x}) = Q(\hat{n}) + iU(\hat{n}) \approx 0.17 \Delta\tau_* \hat{m}^i \hat{m}^{*j} \partial_i v_j \quad (6)$$

where  $\Delta_p$  is the polarization fluctuation,  $Q$  and  $U$  are Stokes parameters,  $\hat{n}$  is the direction of observation (i.e.

<sup>1</sup> <https://spherex.caltech.edu/>

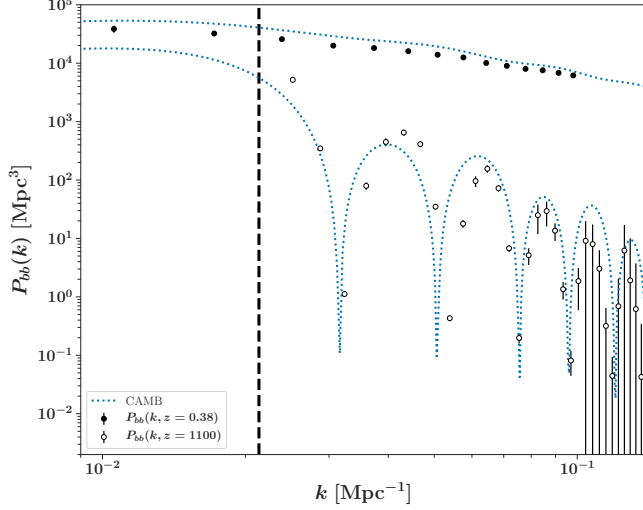


FIG. 1. Baryon power spectra at  $z = 0.38$  (filled-in circles) and  $z = 1100$  (open-circles). The low-redshift power spectrum is derived from Ref. [31]. The high-redshift power spectrum is derived from Ref. [35]’s  $EE$  power spectrum using Equations 12 & 16. As these equations make several simplifying assumptions, the difference between the circles and the spectrum produced by a full treatment by the CAMB code for each redshift (blue dotted line) provides an estimate of the error in the approximation. The black, dashed line gives the acoustic scale, as given by Ref. [10]. All high-redshift curves are arbitrarily normalized.

into the sky),  $\Delta\tau_*$  is the width of the last scattering surface,  $\hat{m}$  is a 2D unit vector on the plane of the sky,  $\hat{m}^*$  is its complex conjugate, and  $v$  is the baryon velocity on the sky<sup>2</sup>.

As an example to gain more intuition, let  $\hat{m} = \hat{x} + i\hat{y}$  and consider  $\hat{n} = \hat{z}$ . Then:

$$Q(\hat{n}) + iU(\hat{n}) \approx 0.17\Delta\tau_* [(\partial_x v_x + \partial_y v_y) + i(\partial_x v_y - \partial_y v_x)] . \quad (7)$$

In other words,  $Q \propto \nabla \cdot v$  and  $U \propto \nabla \times v$ . Note that the velocity due to density perturbations is *irrotational*, which implies that  $U = 0$ . However, this is only for one particular direction (along the  $\hat{z}$ -axis). In general, we must consider all directions on the sky and there will be both  $Q$  and  $U$  polarization.

Now consider the small-angle approximation. Here we specify that all wavevectors,  $\vec{k}$ , are close to our  $\hat{n}$ . In Fourier space, this gives the equation:

$$\Delta_p(\hat{n}, \vec{k}) \approx 0.17\Delta\tau_* ikv_b , \quad (8)$$

where  $k = |\vec{k}|$ . Then, the polarization power spectrum on small scales is:

$$\langle \Delta_p(\hat{n}, \vec{k}) \Delta_p^*(\hat{n}, \vec{k}) \rangle \approx (0.17)^2 \Delta\tau_*^2 k^2 v_b^2 \quad (9)$$

<sup>2</sup> Note that the dipole moment of the CMB temperature gives us the final, radial component of the velocity,  $v_r$ .

Typically, polarization results are reported using  $E$  and  $B$ -modes, which are just a rotation of the  $Q$ - $U$  basis. This basis is specifically chosen such that there are no  $B$ -modes on small scales in the early Universe – instead all of the polarization is given by  $E$ -modes. Thus, the polarization power spectrum is just the  $E$ -mode power spectrum<sup>3</sup>:

$$P_{EE}(k) \approx (0.17\Delta\tau_*)^2 k^2 v_b^2(k) . \quad (10)$$

Now we must connect this equation to the baryon density power spectrum.

Prior to recombination, the baryons and photons can be treated as a single fluid. In a universe with no DM, the behavior is simple inside the horizon:

$$\ddot{\delta}_b + c_s^2 k^2 \delta_b = 0 , \quad (11)$$

where  $\dot{\phantom{x}} \equiv \frac{d}{d\tau}$  (conformal time) and  $c_s$  is the sound speed. In  $\Lambda$ CDM, there would be an additional forcing term on the right-hand side,  $-3\ddot{\Phi}$ , where  $\Phi$  is the cold dark matter potential.

For adiabatic initial conditions, this admits the solution:

$$\delta_b = A(k) \cos(kr_s) , \quad (12)$$

where  $r_s$  is the sound horizon:

$$r_s = \int d\eta c_s , \quad (13)$$

The density can be related to the velocity via the continuity equation. At small scales, we can ignore any changes in the potential and simply treat the baryon-photon fluid as a normal Newtonian fluid. Then the continuity equation in Fourier space is:

$$\dot{\delta}_b(k) + ikv_b(k) = 0 . \quad (14)$$

This gives:

$$v_b = \frac{i}{k} \dot{\delta}_b(k) = -ic_s A(k) \sin(kr_s) . \quad (15)$$

From Equation 10, we have:

$$P_{EE}(k) \approx (0.17\Delta\tau_*)^2 c_s^2 k^2 |A(k)|^2 \sin^2(kr_s) \quad (16)$$

We can find  $A(k)$  using the observed  $EE$  power spectrum and then use Equation 12 to find the density power spectrum. Note that velocity overshoot may shift the peak positions here, but will not change the overall shape of the power spectrum. There is also a small effect

<sup>3</sup> There is an extra term related to fixing the basis for the  $E$ - $B$  decomposition. However, this should be  $\sim 1$  under the small-angle approximation.



from the finite thickness of the last scattering surface – this amplifies scales that are smaller than the thickness of the surface. To account for this effect, we multiply Equation 16 by an exponential factor,  $\exp[k/k_{\Delta\tau_*}]$ , with  $\Delta\tau_* = 19$  Mpc [37].

For the  $EE$  power spectrum, we use the Planck 2018 [35] and the Atacama Cosmology Telescope ACTPol Two Season [38] angular power spectra. We add the data in quadrature. The data is given as multipoles,  $C_l^{EE}$ , of the 2D power spectrum. We must convert this to the 3D power spectrum,  $P_{EE}(k)$ . We approximate  $l = k\eta_* - \frac{1}{2}$ , where  $\eta_*$  is the conformal distance to the last scattering surface<sup>4</sup>[39]. Then, to order unity, the 3D power spectrum is [39, 40]:

$$P_{EE}(k) \sim \frac{\pi l^2}{k^3} C_{l=k\eta_* - \frac{1}{2}}^{EE}. \quad (17)$$

We bin the  $C_l^{EE}$  data into  $l$ -bins with width  $\Delta l = 50$  to increase the signal-to-noise. We also only use  $l \leq 2000$ , due to the high noise in the data above this point.

In Figure 1, we show the baryon power spectrum at  $z = 1100$  and  $z = 0.38$ . As can be seen, the proper dark matter theory must somehow explain how the  $z = 1100$  spectrum smooths out and increases in power on small scales. Note that the BAO ‘wiggles’ in the low-redshift power spectrum look much weaker than those in the CMB-derived spectrum. This is just due to the normal evolution of perturbations over time. Also note that our peaks do not precisely line up with the CAMB<sup>5</sup>-derived peaks at low- $k$ . This occurs because we ignore the cold dark matter driving-term in the continuity equation, which is more prominent at low- $k$  (i.e. velocity overshoot; cf. [21, 41, 42]).

We also indicate the acoustic scale by the dashed, black line on all plots in this paper. We use the Ref. [10] value for the sound horizon size at the drag epoch,  $r_d = 147.09$  Mpc and the comoving distance to this time,  $\eta_*$ , to set  $l_* = \pi\eta_*/r_s$ . Finally, we obtain the  $k$  value using  $k_* = l_*/\eta_* - \frac{1}{2}$ .

### Constraining the form of linearly modified gravity theories

We will now derive the transfer and Green’s functions for the modified gravity theory. We only use the data

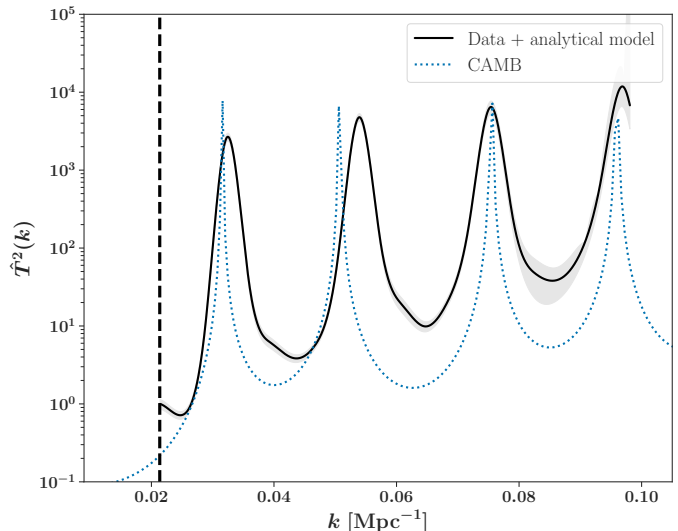


FIG. 2. Baryon transfer function from  $z = 1100$  to  $z = 0.38$ . The black line shows the transfer function computed by applying the analytical model for the  $EE$  power spectrum to the Planck data and combining it with the large-scale structure data. The blue, dotted line shows the transfer function computed assuming  $\Lambda$ CDM. The difference between the two shows the limitations of the analytical approximation used to derive the Green’s function. The gray region shows the  $1\text{-}\sigma$  error from the data. Any alternative gravity theory must predict something close to this transfer function if it is to explain how the fluctuations in the baryon density traced by the polarization signal at  $z \sim 1100$  evolve to the galaxy density field seen at low redshift.

from each survey where they both overlap in  $k$ . This range,  $k \sim 0.01 - 0.1 \text{ Mpc}^{-1}$ , corresponds to small scales (i.e. much smaller than the horizon) today and at recombination.

The transfer function is shown in Figure 2. We also include the CAMB-derived transfer function, which we derive by taking the baryon power spectrum at the same redshifts as our data and dividing them. The transfer function makes the exact evolution of perturbations needed apparent. Power should grow the most on small scales and should oscillate to smooth out the baryon acoustic oscillations. This aligns with the standard  $\Lambda$ CDM picture.

We show the associated Green’s function, computed using the `hankel` python package<sup>6</sup>, in Figure 3. Because the transform includes an integral over all  $k$ -modes, the exact form of the Green’s function depends on the behavior of the transfer function outside of our data range. For the purposes of determining the Green’s function, we need to extrapolate the high- $k$  range as it determines the small- $r$  behavior. We cannot directly probe

<sup>4</sup> This does require setting a cosmology. We use the measured distance to the last scattering surface from Ref. [10]. Since we require that the modified gravity must also fit the measured distance-redshift relation, the distance from last scattering cannot deviate too wildly from the Planck value. In principle, it may be possible to set  $\eta_*$  without setting a cosmology – instead, we might be able to use the alignment of the peaks in each of the power spectra.

<sup>5</sup> <https://camb.info/>

<sup>6</sup> <https://github.com/steven-murray/hankel>

this with our current data and so we try a few different assumptions: 1)  $T^2(k > k_{\text{max}}) = 0$  (solid, black line); 2)  $T^2(k > k_{\text{max}}) = T^2(k_{\text{max}})$  (dotted, black line). These assumptions mostly change the height and phase of the secondary peaks in the Green's function.

Regardless of the assumptions at high- $k$ , the Green's function changes sign near the BAO scale. The Green's function shows the response a modified gravity theory of dark matter must have in order to explain the evolution of baryons on large scales. Thus, any alternative gravity theory would need to: 1) contain this scale to suppress the BAO features over time – changing them from dominant at  $z \sim 1100$  to very low amplitude at  $z \sim 0.4$ ; and 2) have an acceleration law that changes sign around this scale.

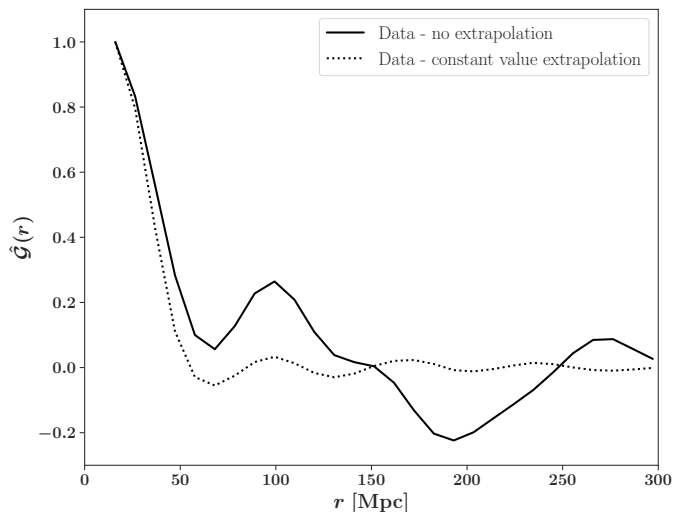


FIG. 3. Green's function for the baryon-only transfer function in Figure 2. The shape at small scales depends on the assumed shape of the transfer functions at  $k \gtrsim 0.1 \text{ Mpc}^{-1}$ . The solid, black line shows the results when we set the values in this range to 0. The dotted, black line gives the results if we set  $T^2(k > k_{\text{max}}) = T^2(k = k_{\text{max}})$ . The errors are dominated by the extrapolation choice, thus we exclude the statistical error bars.

## CONCLUSIONS

Cosmological observations place strong constraints on the form of any modification to General Relativity. In the absence of dark matter, the modified theory must explain how density fluctuations grow from the electron velocity field traced by the CMB polarization at  $z = 1100$  to the galaxy density field seen in the local universe. In this paper, we show that any theory that depends linearly on the density field must have the peculiar Green's function shown in Figure 3.

Modified Newtonian dynamics (MOND) [43] and emergent gravity (EG) [44] both predict that gravity behaves

as predicted by GR at early times and deviates from GR at weak acceleration (MOND) or when dark energy plays an important role (EG). If they are similar to GR at early times, they would both seem to predict significant deviations from the CMB fluctuation spectrum as they do not contain any dark matter. Neither of these theories have cosmologies associated with them, so it is difficult to definitively apply any cosmological test. If we try to compare them to the constraints on the growth rate of structure discussed in this paper, their Newtonian forms at large scales do not seem promising. The accelerations from point sources in both theories scale as  $\sim 1/R$  and this form is often evoked on cosmological scales [45, 46]. This would then predict a power-law Green's function: nothing like what is needed to fit the cosmological observations. In particular, neither predict a special scale at the BAO scale or oscillating acceleration signature. Perhaps, mode-mixing at early times could allow for this to be remedied [24]; however, it is unclear how this could occur while still leading to the  $1/R$  force law and not defying primordial non-Gaussianity constraints.

Perhaps it is possible to use the Green's function of the form found above to find a modified gravity theory that can fit cosmological constraints and all other GR tests. However, given the extreme form of the function, it is not clear that this is possible – in particular, the sign changes would induce quite extreme dynamics within the local volume. CDM remains the simplest explanation for the growth of structure.

We would like to thank Chen Heinrich and Michael Strauss for helpful discussions and feedback on the manuscript. KP received support from the National Science Foundation Graduate Research Fellowship Program under grant DGE-1656466. This work was done as a private venture and not in KP's capacity as an employee of the Jet Propulsion Laboratory, California Institute of Technology.

*Software:* Astropy [47, 48], CAMB [49], Hankel [50], Matplotlib [51], Numpy [52], Pandas [53, 54], SciPy [55] & Seaborn [56].

The software to reproduce the analysis and plots in this paper can be found at: [https://github.com/kpardo/mg\\_bao/](https://github.com/kpardo/mg_bao/).

---

\* [kpardo@caltech.edu](mailto:kpardo@caltech.edu)

- [1] F. Zwicky, *Helvetica Physica Acta* **6**, 110 (1933).
- [2] J. Einasto, A. Kaasik, and E. Saar, *Nature* **250**, 309 (1974).
- [3] V. C. Rubin, J. Ford, W. K., and N. Thonnard, *ApJ* **225**, L107 (1978).
- [4] A. Bosma, *The distribution and kinematics of neutral hydrogen in spiral galaxies of various morphological types*, Ph.D. thesis, - (1978).
- [5] V. C. Rubin, J. Ford, W. K., and N. Thonnard, *ApJ*

- 238**, 471 (1980).
- [6] J. P. Ostriker, P. J. E. Peebles, and A. Yahil, *ApJ* **193**, L1 (1974).
  - [7] J. A. Tyson, F. Valdes, and R. A. Wenk, *ApJ* **349**, L1 (1990).
  - [8] D. M. Wittman *et al.*, *Nature* **405**, 143 (2000), [arXiv:astro-ph/0003014 \[astro-ph\]](#).
  - [9] D. N. Spergel *et al.*, *ApJS* **148**, 175 (2003), [arXiv:astro-ph/0302209 \[astro-ph\]](#).
  - [10] Planck Collaboration *et al.*, *arXiv e-prints*, [arXiv:1807.06209](#) (2018), [arXiv:1807.06209 \[astro-ph.CO\]](#).
  - [11] E. Aprile *et al.* (Xenon Collaboration), *Phys. Rev. Lett.* **121**, 111302 (2018), [arXiv:1805.12562 \[astro-ph.CO\]](#).
  - [12] E. Aprile *et al.* (XENON Collaboration), *Phys. Rev. Lett.* **123**, 251801 (2019).
  - [13] C. M. Will, *Theory and Experiment in Gravitational Physics* (Cambridge University Press, 1993).
  - [14] B. P. *et al.* Abbott, *Phys. Rev. Lett.* **123**, 011102 (2019), [arXiv:1811.00364 \[gr-qc\]](#).
  - [15] B. P. *et al.* Abbott, *ApJ* **848**, L13 (2017), [arXiv:1710.05834 \[astro-ph.HE\]](#).
  - [16] K. Pardo, M. Fishbach, D. E. Holz, and D. N. Spergel, *J. Cosmology Astropart. Phys.* **2018**, 048 (2018), [arXiv:1801.08160 \[gr-qc\]](#).
  - [17] M. Lagos, M. Fishbach, P. Landry, and D. E. Holz, *Phys. Rev. D* **99**, 083504 (2019), [arXiv:1901.03321 \[astro-ph.CO\]](#).
  - [18] M. Ishak, *Living Reviews in Relativity* **22**, 1 (2019), [arXiv:1806.10122 \[astro-ph.CO\]](#).
  - [19] E. M. Lifshitz, *Zhurnal Eksperimentalnoi i Teoreticheskoi Fiziki* **16**, 587 (1946).
  - [20] P. J. E. Peebles and J. T. Yu, *ApJ* **162**, 815 (1970).
  - [21] R. A. Sunyaev and Y. B. Zeldovich, *Ap&SS* **9**, 368 (1970).
  - [22] J. R. Bond and G. Efstathiou, *ApJ* **285**, L45 (1984).
  - [23] P. J. E. Peebles, *ApJ* **284**, 439 (1984).
  - [24] S. S. McGaugh, *ApJ* **611**, 26 (2004), [arXiv:astro-ph/0312570 \[astro-ph\]](#).
  - [25] S. Dodelson, *International Journal of Modern Physics D* **20**, 2749 (2011), [arXiv:1112.1320 \[astro-ph.CO\]](#).
  - [26] Planck Collaboration *et al.*, *arXiv e-prints*, [arXiv:1905.05697](#) (2019), [arXiv:1905.05697 \[astro-ph.CO\]](#).
  - [27] A. Slosar *et al.*, *J. Cosmology Astropart. Phys.* **2008**, 031 (2008), [arXiv:0805.3580 \[astro-ph\]](#).
  - [28] O. Doré *et al.*, *arXiv e-prints*, [arXiv:1412.4872](#) (2014), [arXiv:1412.4872 \[astro-ph.CO\]](#).
  - [29] A. de Graaff, Y.-C. Cai, C. Heymans, and J. A. Peacock, *A&A* **624**, A48 (2019), [arXiv:1709.10378 \[astro-ph.CO\]](#).
  - [30] V. Springel *et al.*, *MNRAS* **475**, 676 (2018), [arXiv:1707.03397 \[astro-ph.GA\]](#).
  - [31] F. Beutler *et al.*, *MNRAS* **455**, 3230 (2016), [arXiv:1506.03900 \[astro-ph.CO\]](#).
  - [32] D. J. Eisenstein *et al.*, *AJ* **142**, 72 (2011), [arXiv:1101.1529 \[astro-ph.IM\]](#).
  - [33] K. S. Dawson *et al.*, *AJ* **145**, 10 (2013), [arXiv:1208.0022 \[astro-ph.CO\]](#).
  - [34] S. Alam *et al.*, *ApJS* **219**, 12 (2015), [arXiv:1501.00963 \[astro-ph.IM\]](#).
  - [35] Planck Collaboration *et al.*, *arXiv e-prints*, [arXiv:1907.12875](#) (2019), [arXiv:1907.12875 \[astro-ph.CO\]](#).
  - [36] M. Zaldarriaga and D. D. Harari, *Phys. Rev. D* **52**, 3276 (1995), [arXiv:astro-ph/9504085 \[astro-ph\]](#).
  - [37] B. Hadzhiyska and D. Spergel, *Phys. Rev. D* **99**, 043537 (2019), [arXiv:1808.04083 \[astro-ph.CO\]](#).
  - [38] T. Louis *et al.*, *J. Cosmology Astropart. Phys.* **2017**, 031 (2017), [arXiv:1610.02360 \[astro-ph.CO\]](#).
  - [39] M. Loverde and N. Afshordi, *Phys. Rev. D* **78**, 123506 (2008), [arXiv:0809.5112 \[astro-ph\]](#).
  - [40] J. R. Bond and G. Efstathiou, *MNRAS* **226**, 655 (1987).
  - [41] W. H. Press and E. T. Vishniac, *ApJ* **236**, 323 (1980).
  - [42] W. Hu and N. Sugiyama, *Phys. Rev. D* **51**, 2599 (1995), [arXiv:astro-ph/9411008 \[astro-ph\]](#).
  - [43] M. Milgrom, *ApJ* **270**, 365 (1983).
  - [44] E. Verlinde, *SciPost Physics* **2**, 016 (2017), [arXiv:1611.02269 \[hep-th\]](#).
  - [45] A. Nusser, *MNRAS* **331**, 909 (2002), [arXiv:astro-ph/0109016 \[astro-ph\]](#).
  - [46] C. Llinares, A. Knebe, and H. Zhao, *MNRAS* **391**, 1778 (2008), [arXiv:0809.2899 \[astro-ph\]](#).
  - [47] Astropy Collaboration *et al.*, *A&A* **558**, A33 (2013), [arXiv:1307.6212 \[astro-ph.IM\]](#).
  - [48] A. M. Price-Whelan *et al.*, *AJ* **156**, 123 (2018).
  - [49] A. Lewis, A. Challinor, and A. Lasenby, *ApJ* **538**, 473 (2000), [arXiv:astro-ph/9911177 \[astro-ph\]](#).
  - [50] S. Murray and F. Poulin, *The Journal of Open Source Software* **4**, 1397 (2019), [arXiv:1906.01088 \[astro-ph.IM\]](#).
  - [51] J. D. Hunter, *Computing in Science & Engineering* **9**, 90 (2007).
  - [52] T. E. Oliphant, *A guide to NumPy*, Vol. 1 (Trelgol Publishing USA, 2006).
  - [53] T. pandas development team, *pandas-dev/pandas: Pandas* (2020).
  - [54] Wes McKinney, in *Proceedings of the 9th Python in Science Conference*, edited by Stéfan van der Walt and Jarrod Millman (2010) pp. 56 – 61.
  - [55] P. Virtanen *et al.*, *Nature Methods* <https://doi.org/10.1038/s41592-019-0686-2> (2020).
  - [56] M. Waskom *et al.*, *mwaskom/seaborn: v0.8.1* (september 2017) (2017).